Organic & Biomolecular Chemistry

Accepted Manuscript

ROYAL SOCIETY OF CHEMISTRY

www.rsc.org/obc

Journal Name

RSCPublishing

ARTICLE

Hydrolytic inhibition of α-chymotrypsin by 2,8,14,20-tetrakis(D-leucyl-D-valinamido)resorc[4]arenecarboxylic acid: a spectroscopic NMR and computational combined approach

Cite this: DOI: 10.1039/xoxxoooooox

Received ooth January 2012,
Accepted ooth January 2012

DOI: 10.1039/xoxxoooooox

www.rsc.org/

Gloria Uccello-Barretta,[a*] Federica Balzano,[a] Federica Aiello,[a] Letizia Vanni,[a] Mattia Mori,[b] Sergio Menta,[c] Andrea Calcaterra[c] and Bruno Botta[c]

The stereochemical features of 2,8,14,20-tetrakis(D-leucyl-D-valinamido)resorc[4]arenecarboxylic acid and *N*-succinyl-L-alanyl-L-alanyl-L-prolyl-L-phenylalanine-4-nitroanilide polypeptide substrate were investigated by Nuclear Magnetic Resonance spectroscopy. Proton selective relaxation parameters gave the basis of the inhibitory activity of resorcin[4]arene in the hydrolysis of polypeptide substrate by α-chymotrypsin. Results showed that an interaction between the resorcin[4]arene and α-chymotrypsin does occur, and involves the hydrophobic moiety of the macrocycle. This interaction is further reinforced by polar groups located on the side chains of the resorcin[4]arene, whereas the macrocycle/polypeptide substrate interaction is negligible. Conformational analysis and interaction studies carried out by molecular modeling are in good agreement with the NMR data, thus providing an additional support to the rationalization of the inhibitory potential of resorcin[4]arenes on α-chymotrypsin activity.

Introduction

Protein-protein interaction plays a well-recognized role in many biological processes,[1] and constitutes the basis for the development of new synthetic receptors capable of binding to protein surface, thus inhibiting their active sites involved in biological mechanisms.[2] The inactivation process could be determined by the formation of covalent interactions, which irreversibly modify the protein, or non-covalent ones, which allow the complete recovery of the structure and the activity of the protein.

Multidentate ligands,[3] small molecules[4] or macrocyclic compounds, such as porphyrins[5] and calix[4]arenes,[6] have been developed as inhibitors of the protein-protein interaction. Recently, calix[4]arenes and resorcin[4]arenes endowed with dipeptidic chains have been proposed as protein inhibitors.[7-9] The possibility of preselecting their conformational and structural features by means of macrocycles flexibility and aminoacidic sequence provides the opportunity of modulating their inhibiting properties. Indeed, the presence of *N*- or *C*-linked peptidic chains confers important properties to the macrocycles, including the ability to recognize proteins and carbohydrates and the possibility to form stable inclusion complexes. In particular, *N*-linked peptidoresorcin[4]arenes have been probed in the inhibition of hydrolytic activity of α-chymotrypsin by in vitro assays,[7a] as in the case of calix[4]arenes.[10]

In order to point out the stereochemical basis of the inhibitory activity of *N*-linked peptidoresorcin[4]arenes, the potentialities of Nuclear Magnetic Resonance (NMR) spectroscopy in the study of molecular recognition phenomena were exploited. Among already reported[7a] resorcin[4]arenes with proved α-chymotrypsin inhibitory potential, 2,8,14,20-tetrakis(D-leucyl-D-valinamido)resorcin[4]arenecarboxylic acid (**1**-DD, Fig. 1) was selected, for its better water solubility, as inhibitor of the hydrolysis of *N*-succinyl-L-alanyl-L-alanyl-L-prolyl-L-phenylalanine-4-nitroanilide (Suc-AAPF-pNA, Fig. 1) by α-chymotrypsin (ChT). Starting from the definition of the stereochemistry of both **1**-DD and Suc-AAPF-pNA in polar solvents, binary mixtures resorcin[4]arene/ChT and resorcin[4]arene/Suc-AAPF-pNA were investigated. The study required the use of techniques of detection of through space dipolar interactions based on ROE (Rotating-frame Overhauser Enancement)[11] and proton selective relaxation rates measurements[12] as well as techniques for detecting the translational diffusion (DOSY, Diffusion Ordered SpectroscopY),[13] which are strongly sensitive to complexation phenomena.

Journal Name RSCPublishing

ARTICLE

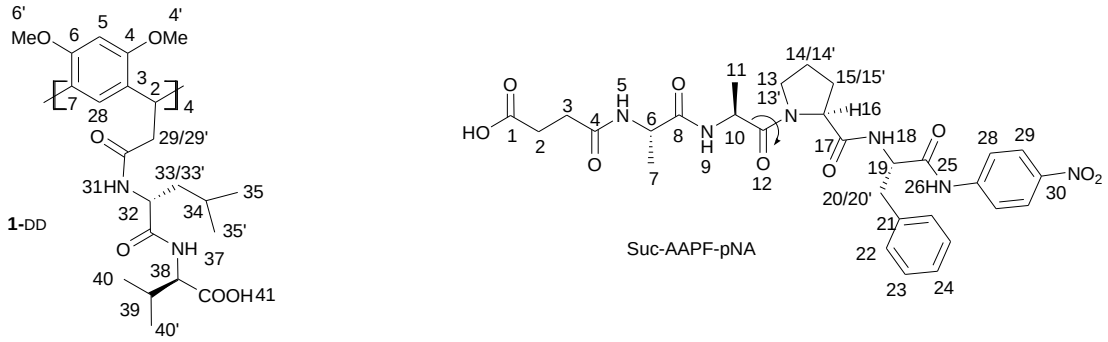

Fig 1. Resorcin[4]arene **1**-DD and Suc-AAPF-pNA structures with numbering scheme for NMR analysis.

NMR-based investigations were complemented by molecular modeling studies of the **1**-DD/ChT interaction. Since **1**-DD has many degrees of freedom, especially within the dipeptide chains connected to the resorcin[4]arene macrocyclic core, exhaustive sampling provided by conformational analysis coupled with molecular docking and energy minimization of the **1**-DD/ChT adduct was performed to identify the most probable binding conformation of **1**-DD to ChT.

Results and discussion

Stereochemical analysis by NMR

The stereochemical features of **1**-DD and Suc-AAPF-pNA were ascertained not only in buffered D_2O, but also in DMSO-d_6, which allowed a better conformational definition, mainly regarding the stereochemical features of the amide fragments. The detailed description of NMR results regarding the conformational analysis of the two compounds is reported in Supplementary Information.

1-DD. Preliminarily, the possible occurrence of self-aggregation processes was ruled out by comparing the ^{1}H NMR chemical shifts and diffusion coefficients of **1**-DD in DMSO-d_6 solutions progressively diluted from 10 mM to 0.1 mM. Interestingly, the diffusion coefficient of **1**-DD is comparable with that measured for analogues resorcin[4]arenes in the same solvent.[14] On these bases, the dipolar interactions detected in the ROESY maps were reliably attributed to intramolecular effects.

The prevalence of the cone conformation of **1**-DD (Fig. 2) has been ascertained in DMSO-d_6 solution, with the dipeptide chains in an unfolded conformation, which elongates outwards the cone structure. The methylene protons H-29/29' are directed towards the lower rim of the resorcin[4]arene. The alkyl part of the *N*-linked leucine fragment is in front of the aromatic moieties and in proximity of its upper rim, with its amide proton NH-31 directed at the lower rim and hence pointing at methylene protons H-29/29'. In the valine residue, the amide proton NH-37 is oriented at the upper rim and faced to the bond CH-32 of the leucine fragment; its alkyl group is far away from the resorcin[4]arene structure. Inside each amino acid fragment, the adjacent NH and CH bonds are reciprocally transoid, as demonstrated on the basis of the very weak ROE effects detected between each NH proton and its vicinal CH proton, in comparison with other dipolar interactions at the frequencies of H-29/29' in the case of NH-31 (Fig 2Sg) and H-32 in the case of NH-37 (Fig. 2Sh).

H-D exchange does not allow us to detect amide protons in D_2O solutions, thus limiting the conformation definition.

However the most significant difference detected in D_2O regards the occurrence of a rotation about the C2-C29 bond, which strongly perturbs both chemical shifts and vicinal coupling constants of the protons belonging to the same fragment. The methylene proton H-29' points at the upper rim being faced to methine proton H-2 and the other proton H-29 is directed at the lower rim (Supplementary Information). It is to note that in DMSO-d_6 the two protons are isochronous.

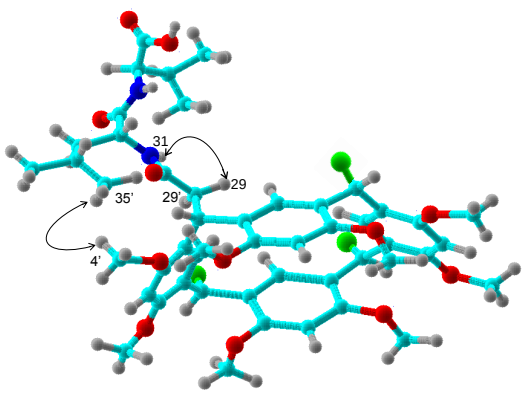

Fig. 2. Three-dimensional representation of **1**-DD according to NMR data collected in DMSO-d_6: the most important ROE effects for the conformational analysis are highlighted. Only one dipeptidic chain is represented; the other chains are indicated with green balls.

Suc-AAPF-pNA. As in the case of **1**-DD, the possible occurrence of self-aggregation processes was ruled out by DOSY experiments and ^{1}H NMR analyses. The literature[15] describes the coexistence of the *trans-cis* stereoisomers of Suc-

AAPF-pNA, which are originated by the rotation about the Pro-Ala bond (pointed out in Fig. 1). The two species are distinguished in the ^{1}H NMR spectrum (Figure 6S) in the ratio 90 to 10, respectively. Signals of the minor isomer (*cis*) were assigned by exploiting the exchange cross-peaks, which could be detected in the 2D ROESY maps. For the conformational analysis, we assumed the expected *trans* NH-CO stereochemistry inside each amide bond. Starting from this premise, the conformation of the *trans* stereoisomer of Suc-AAPF-pNA is depicted in the Fig. 3. With respect to the plane of the pentatomic proline ring, the NH-18 of Phe, the carbonyl group of the p-nitroanilide moiety (C-25), the carbonyl C-12 and NH-9 of Ala adjacent to Pro and methine H-6 of the terminal Ala residue all are on the same half-plane which contains H-16 of the pentatomic ring. NH-5, carbonyl C-8 and methyl H-11, on one side, and carbonyl C-17, H-19 and NH-26, on the other one, must lie on the opposite half-plane (for major details, see Supplementary Information). The methine proton H-10 points at the methylene protons H-13/13' of the pentatomic ring with the methyl H-11 farther from the two protons. The benzyl group of Phe is located between the two arms, whereas the p-nitroanilide moiety is external with respect to them. A further refinement of the conformational data was achieved by means of proton selective relaxation rates measurements, which are described in the Supplementary Information.

As probes of the conformational changes occurring in the *cis* stereoisomer, due to the rotation about the Ala-Pro bond, we selected the protons H-18 and H-19. Their resonances were well differentiated from the corresponding resonances of the prevailing stereoisomer and not superimposed to other signals. Relaxation rates of the two protons remarkably increased as the consequence of the rotation about the Ala-Pro linkage, bringing the amide proton H-18 of Phe and the amide proton H-9 of Ala in close proximity (a very short distance of 1.94 Å was calculated by means of proton selective relaxation rates measurements, see Supplementary Information). Therefore, the two side arms of Pro fragment were in spatial proximity in the *cis* stereoisomer (Fig. 3).

Spectral parameters in D_2O are very similar to those in DMSO-d_6, which suggested that also the conformational features in the two solvents should be similar (see Supplementary Information).

Resorcin[4]arene/chymotrypsin and resorcin[4]arene/Suc-AAPF-pNA interactions

Starting from the knowledge of the stereochemical features of the resorcin[4]arene and the substrate Suc-AAPF-pNA, we faced the problem of the complexation phenomena originated by the resorcin[4]arene.

A very high ligand to macromolecule ratio is mandatory for ligand/macromolecule interaction investigations by NMR to obtain a detectable signal for the ligand. Therefore, highly sensitive NMR parameters must be selected. Among them, the most suitable are relaxation rates.[16]

In particular, it has been shown that the selective relaxation rate (R^{ms}) of the ligand is a more sensitive indicator of binding than non-selective rate (R^{ns}) is. In fact, methods based on the determination of the selective relaxation rates take advantage of the favourable dependence of R^{ms} on the correlation time (τ_c) in the region of slow molecular motions, in which the small molecule is forced by the interaction with the macromolecule. In the fast-motion region ($\omega^2\tau_c^2 \ll 0.6$; ω = Larmor frequency), both the selective (R^{ms}) and non-selective (R^{ns}) relaxation rates increase progressively with increasing τ_c. When the molecular motion of the ligand is slowed down to the $\omega^2\tau_c^2 \gg 0.6$ region, as a consequence of the interaction with the macromolecule, R^{ms} shows a sharp increase, whereas R^{ns} reaches a maximum for $\omega^2\tau_c^2 \cong 0.6$ and then decreases with further increasing of $\omega^2\tau_c^2$. In the fast-exchange limit, the measured relaxation rates (R_{obs}) are the weighted means of the values in the bound (R_b) and free (R_f) states (Eq. 1).

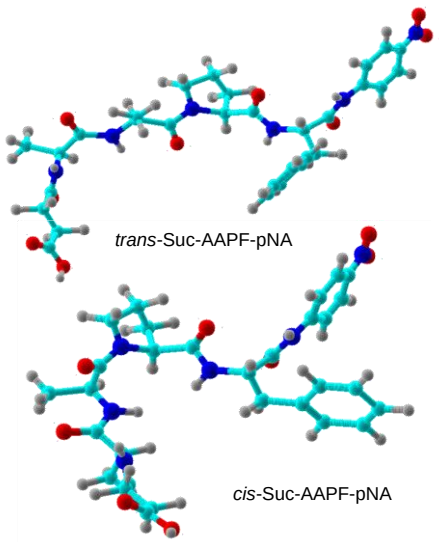

Fig. 3. Three-dimensional representation of the two isomers of Suc-AAPF-pNA according to NMR data.

$$R_{obs} = R_f x_f + R_b x_b \qquad (1)$$

where x_b and x_f are the molar fractions of the bound and free species. As the concentration of the ligand is much higher than that of the macromolecule, then $x_f \cong 1$, and

$$R_{obs} = R_f + R_b x_b \qquad (2)$$

For the 1 to 1 complexation macromolecule (M)/ligand (L) equilibrium, where [L] » [M], Eq. 1 can be expressed as follows:

$$R_{obs} = \frac{KR_b[M_0]}{1+K[L]} + R_f \qquad (3)$$

where K is the heteroassociation constant and $[M_0]$ is the initial macromolecule concentration. The plot of R_{obs} *vs* $[M_0]$ should give a straight line, the slope of which is defined as "affinity index" ([A]),[17] a parameter which depends on the temperature and ligand concentration (Eq. 4).

$$[A] = \frac{KR_b}{1+K[L]} \qquad (4)$$

In case of n binding sites of equal strength, the affinity index takes different forms, but in any situation, the relationship between R_{obs} and $[M_0]$ is always linear (Eq. 5), and thus the parameter [A] is independent of the complexation

stoichiometry and constitutes a powerful tool for comparing the ligand-macromolecule affinities.

$$R_{obs} = R_f + [A][M_0] \qquad (5)$$

Different sites of the molecule can have different affinity indexes, which must be normalized on the basis of the respective selective relaxation rates in the free states (R_f). Thus, a normalized affinity index $[A^N]$[18] can be obtained (Eq. 6), which provides a measure of ligand-macromolecule global affinity.

$$[A^N] = \frac{[A]}{R_f} \qquad (6)$$

Resorcin[4]arene/substrate. In view of the very limited solubility of the substrate Suc-AAPF-pNA in an aqueous medium, a maximum of five equivalents of Suc-AAPF-pNA could be solubilized in D_2O in the mixtures containing **1**-DD 1.70 mM. Normalized proton selective relaxation rates of **1**-DD were scarcely sensitive to the presence of the substrate with the unique exception of the proton H-38, adjacent to the terminal carboxyl function (Table 1).

Table 1. Normalized selective relaxation rates ($\Delta R/R_f$, where $\Delta R=R_{obs}-R_f$) of selected protons of **1**-DD (1.70 mM, D_2O, pH 7.4) in the presence of Suc-AAPF-pNA (8.37 mM, **1**-DD/Suc-AAPF-pNA 1:5).

$\Delta R/R_f$									
H_5	H_2	H_{29}	$H_{29'}$	H_{32}	$H_{33\text{-}33'}$	H_{34}	$H_{35'}$	H_{38}	H_{39}
0.06	0.08	0.09	0.06	0.03	0.17	0.02	0.08	0.28	0.15

Resorcin[4]arene/enzyme. Resorcin[4]arene/enzyme mixtures were analysed in D_2O by NMR with **1**-DD 1.68 mM and changing ChT from 0.016 mM (**1**-DD/ChT ≈ 100:1) till to 0.074 mM (**1**-DD/ChT ≈ 22:1).

The relaxation rates of the resorcin[4]arene significantly increase in the mixture **1**-DD/ChT starting from the ratio 35 to 1. The degree of perturbation of the protons of **1**-DD shows a linear dependence on enzyme concentration gradients, as shown in Fig. 4, and it is well described by the normalized affinity index (Table 2).

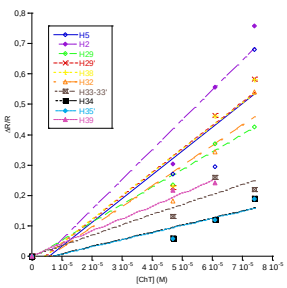

Fig. 4. Dependence of the normalized selective relaxation rates of **1**-DD protons (1.68 mM, D_2O) on the ChT concentration.

The hydrophobic component of **1**-DD, consisting of the aromatic rings mutually concatenated, is the molecular portion involved more effectively in the interaction with the enzyme. In fact, the aromatic proton H-5 and the methine proton H-2 on the resorcin[4]arene bridge were involved more extensively in the interaction with the enzyme. Interestingly, the two anisochronous methylene protons H-29 and H-29' showed also well-differentiated affinity indexes: H-29', which is cisoid to H-2, has enhanced affinity for the enzyme with respect to H-29 which is *trans* to it and, hence, directed towards the lower rim of the resorcin[4]arene.

Table 2. Mono-selective relaxation rates of selected protons of **1**-DD (1.68 mM, D_2O, 25 °C) in the free state (R_f, s^{-1}) and in the mixture **1**-DD/ChT 22:1 (R_{obs}, s^{-1}), corresponding values of normalized relaxation rates ($\Delta R/R_f$, where $\Delta R=R_{obs}-R_f$) and normalized affinity indices ($[A^N]$, M^{-1}).

Proton	$\Delta R/R_f$	$[A^N]$
5	0.63	8319
2	0.76	10621
29	0.43	5873
29'	0.59	8123
32	0.56	5989
33-33'	0.56	3756
34	0.22	4950
35'	0.19	2360
38	0.40	7613
39	0.47	5679

The literature[19] shows that the catalytic triad, which is involved in the mechanism of hydrolysis by the chymotrypsin, is composed of the three amino acids serine, histidine and aspartate. Therefore, once established that the resorcin[4]arene is capable of interacting with the enzyme, the ability of **1**-DD to interact with the above amino acids was also evaluated by analysing solutions containing the individual amino acids, their binary mixtures and the ternary mixture. The resorcin[4]arene was analysed dissolved in DMSO-d_6 (10 mM), with the amino acids (10 mM each) dissolved in the minimum amount of buffered water (10 μL for Ser, 30 μL for His and 50 μL for Asp, D_2O, phosphate buffer, pH = 7.4).

The ability of each amino acid to associate with the other amino acids or with the resorcin[4]arene was investigated by measuring their diffusion coefficients, which are expected to undergo detectable decreases as the consequence of the occurrence of complexation processes.

In all cases, the effect of changes in viscosity of the medium due to the presence of the solutes, and, more importantly, the effect of the presence of D_2O in mixture with the DMSO-d_6 on the diffusion coefficients were verified. TMS was employed as an internal standard for viscosity,[20] by comparing its diffusion coefficient in the different solutions to that one of pure TMS in DMSO-d_6. In no cases, variations of the diffusion coefficient of TMS attributable to the presence of the solutes were detected. On the contrary, the addition of D_2O to DMSO-d_6 was responsible for relevant variations of the diffusion coefficient of TMS (Table 6S, Supplementary Information). As an example, on varying the DMSO-d_6/D_2O ratio from 70:1 to 7.8:1 (corresponding to the addition of 10 and 90 μL of D_2O, respectively) the diffusion coefficient of the TMS decreases from 5.5 x 10^{-10} m^2s^{-1} to 4.0 x 10^{-10} m^2s^{-1}. Therefore, all the diffusion coefficients were corrected, using the appropriate correction factor determined on the basis of TMS diffusion coefficients ratios.

First, the ability of the three amino acids to give rise to mutual interactions was evaluated. For the three amino acids Ser, His and Asp, the diffusion coefficients of 2.6 x 10^{-10} m^2s^{-1}, 3.2 x 10^{-10} m^2s^{-1} and 2.7 x 10^{-10} m^2s^{-1} were, respectively, measured (Table 3). On adding His to Ser, the diffusion coefficients of the two amino acids decreased up to 2.5 x 10^{-10} m^2s^{-1} (Ser) and 2.6 x 10^{-10} m^2s^{-1} (His). The addition of Asp to the mixture of the two amino acids caused further reduction of the diffusion coefficients of Ser and His, but the diffusion coefficient of Asp remained unchanged (Table 3).

Table 3. Diffusion coefficients (D, x 10^{10} m^2s^{-1}, DMSO-d_6, 25 °C) calculated for free ammino acids (D_f) and for their binary, ternary and quaternary mixtures (D_{obs}) in the absence and in the presence of **1**-DD (10 mM).

		D_{obs}				
	D_f	Ser/His	Ser/His/ Asp	**1**-DD/ Ser	**1**-DD/ Ser/His	**1**-DD/Ser/ His/Asp
Ser	2.6	2.5	2.2	1.9	2.6	1.6
His	3.2	2.6	2.0		1.1	1.6
Asp	2.7		2.7			2.9

Therefore, serine and histidine associate unlike aspartate, which has no tendency to aggregate with the two amino acids, but it favours their mutual interaction. This result is in agreement with literature data.[19]

The effect of the resorcin[4]arene on the diffusion coefficient of Ser is very marked, in fact in the binary mixture **1**-DD/Ser the diffusion coefficient of 1.9 x 10^{-10} m^2s^{-1} was measured for the amino acid. This trend is however expected, in view of the fact that complexation causes an apparent increase in the size of the complexed species and, therefore, a decrease of the parameter of diffusion according to the Stokes-Einstein equation (Eq. 7).

$$D = \frac{kT}{6\pi\eta r} \qquad (7)$$

Where k is the Boltzmann constant, T the absolute temperature, η the solution viscosity and r is the hydrodynamic radius.

Moreover, in the fast-exchange conditions, the diffusion coefficients of the amino acids in the mixtures with **1**-DD (D_{obs}) are the weighted averages of their value in the free and bound states (D_f and D_b respectively), according to Eq. 8:

$$D_{obs} = D_f x_f + D_b x_b \qquad (8)$$

Therefore, the extent of decrease of the diffusion coefficient is proportional to the degree of complexation of the amino acid. When the molecular sizes of the substrate and of the receptor are highly differentiated, as in our case, then it is reasonable to assume that the motion of diffusion of the amino acid is fully controlled by the receptor. Consequently the bound molar fraction x_b can be calculated by Eq. 9.

$$x_b = \frac{D_{obs} - D_f}{D_b - D_f} \qquad (9)$$

where D_b represents the diffusion coefficient of the complexing agent, the resorcin[4]arene in our case.

Therefore, by approximating the diffusion coefficient of Ser in the bound state to that of **1**-DD (0.91 x 10^{-10} m^2s^{-1}), we calculated the fraction of Ser bound to **1**-DD, which was very high (0.4). The addition of His to the mixture Ser/**1**-DD causes an increase of the diffusion coefficient of Ser (2.6 x 10^{-10} m^2s^{-1}), but a decrease of the diffusion coefficient of His (1.1 x 10^{-10} m^2s^{-1}) with respect to the pure amino acid. The decrease is much more marked than that detected in the mixture Ser/His in the absence of **1**-DD (Table 3). This result shows that **1**-DD interacts more strongly with His compared to Ser. The most interesting result is obtained in the mixture resulting from the addition of Asp to the solution containing the resorcin[4]arene and the two amino acids Ser and His; in fact, a very marked decrease of the diffusion coefficient of Ser was detected. Asp not only does not interact with the macrocycle, but, rather, its diffusion coefficient increases, as well as increases the diffusion coefficient of His. Therefore, aspartate promotes the interaction of serine with the resorcin[4]arene, which, however, requires the cooperation of histidine.

Molecular Modeling

Structural insights on the conformation of **1**-DD and its adduct with ChT were investigated also by means of molecular modeling. To this aim, conformational analysis, molecular docking and energy minimization studies were performed.

Conformational analysis of 1-DD. A rough structure of **1**-DD was built and energy minimized as reported in Experimental section. The Mixed torsional/Low-mode sampling method for conformational search was used to sample the four peptidic side chains of **1**-DD, while the resorcin[4]arene moiety was frozen to maintain the flattened cone conformation obtained by the previous energy minimization. Indeed, resorcin[4]arenes are known to display a symmetric cone conformation in solution, which is the result of the equilibrium between two equivalent forms. Upon interacting with a molecular partner as well as in solid and gas phases, resorcin[4]arenes are characterized only by the so named flattened cone form, as already observed experimentally.[21-23] The 1000 conformers endowed with the lowest total energy were stored for further molecular docking studies.

Molecular docking. **1**-DD conformers were docked towards the crystallographic structure of ChT (PDB ID: 1YPH)[7a] by means of the FRED software (OpenEye).[24] Docking poses were then clustered using a 2 Å RMSD tolerance, giving rise to three different clusters endowed with comparable number of poses and lowest binding energy. The top ranking pose of each cluster was subsequently compared to NMR data through visual inspection. Notably, only one cluster was nicely in agreement with experimental data and the binding mode described thereafter refers to the lowest binding pose of this cluster, relaxed through in depth energy minimization performed with Amber12.[25]

As observed by NMR, the hydrophobic resorcin[4]arene core of **1**-DD is effectively involved in the interaction with the catalytic groove of ChT. Overall, hydrophobic contacts are performed by **1**-DD with Ile99 and Trp215 within the ChT catalytic cleft (Fig. 5) (for the sake of clarity, residues numbering is the same as adopted in the crystallographic structure). This particular positioning of the **1**-DD resorcin[4]arene core occludes the entrance of the catalytic site formed by Ser195, His57 and Asp102, thus providing a possible explanation to the inhibitory activity observed in vitro against ChT.[7a] Notably, protons H-5, H-2 and H-29' that were highlighted by the NMR study as strongly involved in the interaction with ChT (Table 2), are in close proximity with the protein surface.

Hydrophobic contacts are established also by the side chains of dipeptide arms, particularly leucine residues, which interact in small hydrophobic clefts within the catalytic site (i.e. a cleft formed by Ile99, Met180 and Trp215; a second cleft formed by Met192, catalytic residues and Gly216, see also Figure 11S, Supplementary Information). However, principal interaction performed by these arms are of polar nature. Indeed, a network of H-bond and electrostatic interactions with ChT residues of the catalytic triad as well as residues located within the catalytic groove are established. These interactions may contribute to stabilize the **1**-DD/ChT adduct as suggested by spectroscopic data. Notably, molecular modeling showed that the NH-37 proton of a dipeptide arm establishes a H-bond interaction with the side chain of the catalytic Ser195 (Fig. 5), probably contributing to reinforce the inhibitory effect of **1**-DD. As observed by NMR, in DMSO-d_6 NH-37 protons of other dipeptide arms are projected towards the upper rim of the resorcin[4]arene core while protons NH-31 are projected towards the lower rim of **1**-DD and are docked in close

proximity of the protein surface. Additional H-bond interactions are established by the dipeptide chains with Tyr94, Lys175, Gly216, Ser218 and Thr219, while the terminal carboxyl groups perform salt bridges and H-bonds with Gly59, Lys90, Gly193, Ser195, Lys177 and Ser217.
Electrostatic properties of ChT were evaluated by solving the Poisson-Boltzmann equation using APBS. Results are shown in Fig. 6 and further confirm that the resorcin[4]arene core interacts within a hydrophobic region of the ChT catalytic groove, whereas the dipeptide chains and, particularly, C-terminal carboxyl groups, are docked within positively charged regions of ChT.
Finally, the surface of **1**-DD protons H-2, H-5, H-29'and H-32 that were highlighted by NMR studies shows a fine shape complementarity with the surface of ChT catalytic groove (Figure 12S, Supplementary Information), while the two other clusters found by molecular docking do not (data not shown). The good agreement between experimental NMR data and docking results corroborates the reliability of the predicted binding mode of **1**-DD towards ChT and provides further structural insight to the mechanism of ChT inhibition by **1**-DD.

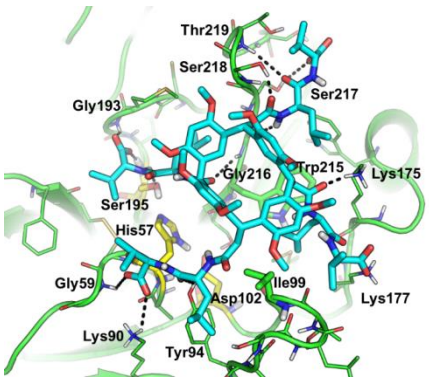

Fig. 5. Docking-based binding mode of **1**-DD towards the catalytic groove of ChT. **1**-DD is shown as cyan sticks, ChT as green cartoon and lines. Catalytic residues Ser195, His57 and Asp102 are shown as yellow sticks; ChT hydrophobic residues interacting with the **1**-DD resorcin[4]arene core are shown as green sticks and labeled. Residues interacting with the dipeptide arms of **1**-DD are also labeled. Polar contacts are highlighted as black dashed lines. Non-polar hydrogen atoms were omitted.

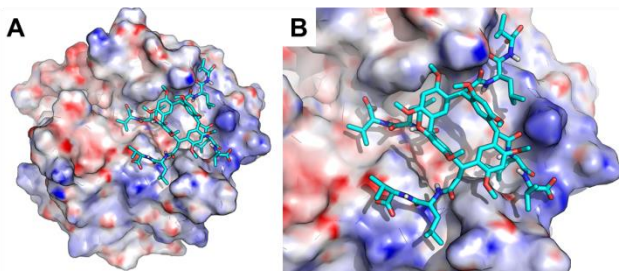

Fig. 6. Electrostatic complementarity between ChT and the docking-based binding mode of **1**-DD. A) ChT surface is coloured according with the electrostatic charge density: blue = positive charge, red = negative charge, white = hydrophobic regions. **1**-DD is shown as cyan sticks, non-polar hydrogen atoms were omitted. B) Magnification of panel A.

Conclusions

The ability of resorcin[4]arene **1**-DD to interact with chymotrypsin rather than Suc-AAPF-pNA has been ascertained as responsible for its inhibitory capability of the hydrolytic activity of the enzyme. Its hydrophobic skeleton constituted by the aromatic rings is predominantly engaged in the interaction with chymotrypsin, thus favouring ancillar hydrophylic interaction of the polar functions of the dipeptide chains which are bent at the upper rim of the resorcin[4]arene.
The dipeptide chains could play a fundamental role in the interaction with the amino acids, which are recognized as responsible for the hydrolysis process, i.e. serine, histidine and aspartate. As a matter of fact, the ability of **1**-DD of interacting with both serine and histidine was demonstrated, which, however, requires the cooperation of aspartate.
Thus, rigidly assembled aromatic moiety in a highly ordered cyclic structure bearing peptide external arms gives a valuable opportunity of achieving a fine tuning of hydrophobic and hydrophilic interactions for the rational design of enzyme inhibitors, which could be eventually exploited also for the controlled release of targeted therapeutic agents.
Finally, the stereochemical assembling of *cis*-Suc-AAPF-pNA may be recognized as responsible for the inability[15] of this stereoisomer to participate to the mechanism of hydrolysis catalyzed by the enzyme. This mechanism probably requires the cooperation of the two chains of Suc-AAPF-pNA linked to proline, which is not possible in *cis*-Suc-AAPF-pNA, where the two side arms are each other in spatial proximity. The two side arms of *cis*-Suc-AAPF-pNA, which have their polar groups involved in reciprocal interactions, are not available for effective interactions with the enzyme.

Experimental

Materials

α-Chymotrypsyn (Type II) from bovine pancreas (ChT), Suc-AAPF-pNA, D-serine, L-histidine, L-aspartate and phosphate buffer were purchased from Sigma Aldrich. Deuterated water (D_2O) and dimethylsulfoxide (DMSO-d_6) were purchased from Deutero GmbH. **1**-DD was synthesized as previously described.[7a]

NMR measurements

NMR measurements were performed on a spectrometer operating at 600 MHz for ^{1}H nuclei. The temperature was controlled to ± 0.1 °C. The 2D NMR spectra were obtained by using standard sequences with the minimum spectral width required. Proton 2D gCOSY (gradient COrrelated SpectroscopY) spectra were recorded with 256-512 increments of 2-16 scans and 2K data points. The relaxation delay was 3 s. 2D TOCSY (TOtal Correlation SpectroscopY) spectra were recorded by employing a mixing time of 80-120 ms. The pulse delay was 1 s; 256-512 increments of 4-64 scans and 2K data points each were collected. The 2D ROESY (Rotating-frame Overhauser Enhancement SpectroscopY) experiments were performed by employing a mixing time ranging from 50 to 600 ms. The pulse delay was 1-5 s; 256-512 increments of 16-64 scans and 2K data points each were collected. 1D ROESY spectra were recorded using the selective pulse SEDUCE generated by means of the Agilent Pandora Software. The selective 1D ROESY spectra were acquired with 512-4096 scans in 32K data points with a 1 s relaxation delay and a mixing time ranging from 50 to 600 ms. gHSQC (gradient Heteronuclear Single Quantum Coherence) and HMBC

(Heteronuclear Multiple Bond Correlation) spectra were recorded by employing a pulse delay of 1 s and 128 or 200 increments of 64-128 scans. HMBC experiments were optimized for a long-range ^{1}H-^{13}C coupling constant of 8 Hz.

DOSY (Diffusion Ordered SpectroscopY) experiments were carried out by using a stimulated echo sequence with self-compensating gradient schemes and 64K data points. Typically, g was varied in 20 steps (2-32 transients each) and Δ and δ were optimized in order to obtain an approximately 90-95% decrease in the resonance intensity at the largest gradient amplitude. The baselines of all arrayed spectra were corrected prior to processing the data. After data acquisition, each FID was apodized with 1.0 Hz line broadening and Fourier transformed. The data were processed with the DOSY macro (involving the determination of the resonance heights of all the signals above a pre-established threshold and the fitting of the decay curve for each resonance to a Gaussian function) to obtain pseudo two-dimensional spectra with NMR chemical shifts along one axis and calculated diffusion coefficients along the other. Gradient amplitudes in DOSY experiments have been calibrated by using a standard sample of D2O 99 %.

The longitudinal selective relaxation rates were measured in the initial rate approximation[26] using the selective pulse IBURP 2 and the inversion recovery sequence with a selective 180-pulse at the selected frequency.

1-DD. ^{1}H NMR (600 MHz, 1.68 mM, D_2O (pH 7.4), 25 °C) δ (ppm): 6.70 (4H, H28, sl); 6.43 (4H, br s, H-5); 4.86 (4H, dd, $J_{2\text{-}29/29'}$ = 11.5 Hz, H-2); 4.05 (4H, dd, $J_{32\text{-}33/33'}$ = 4.9 Hz, H-32); 3.90 (4H, d, $J_{38\text{-}39}$= 5.6 Hz, H-38); 3.53 (24H, s, OMe-4'/6'); 2.79 (4H, dd, $J_{29\text{-}29'}$ = 12.8 Hz, $J_{29\text{-}2}$ = 11.5 Hz, H-29); 2.66 (4H, dd, $J_{29'\text{-}29}$ = 12.8 Hz, $J_{29'\text{-}2}$= 3.1 Hz, H-29'); 1.92 (4H, m, H-39); 1.34 (8H, m, H-33/33'); 1.27 (4H, m, H-34); 0.73 (12H, d, $J_{40\text{-}39}$= 6.0 Hz, H-40); 0.71 (12H, d, $J_{40'\text{-}39}$= 6.0 Hz, H-40'); 0.69 (12H, d, $J_{35\text{-}34}$= 7.1 Hz, H-35); 0.52 (12H, d, $J_{35'\text{-}34}$= 7.1 Hz, H-35').

^{1}H NMR (600 MHz, 10 mM, DMSO-d_6, 25 °C) δ (ppm):12.45 (4H, br s, COOH); 7.96 (4H, br s, H-37); 7.51 (4H, br s, H-31); 6.71 (4H, s, H-28); 6.37 (4H, s, H-5); 4.84 (4H, t, $J_{2\text{-}29}/_{29'}$ = 6.1 Hz, H-2); 4.31 (4H, m, H-32); 4.07 (4H, t, $J_{38\text{-}39}$ = $J_{38\text{-}37}$= 7.1 Hz, H-38); 3.62 (12H, s, OMe4'); 3.58 (12H, s, OMe6'); 2.63 (8H, d, $J_{29/29'\text{-}2}$ = 6.1 Hz, H-29/29'); 1.96 (4H, m, H-39); 1.27 (8H, m, H-33/33'); 1.16 (4H, m, H-34); 0.79 (12H, d, $J_{40\text{-}39}$ = 6.4 Hz, H-40); 0.77 (12H, d, $J_{40'\text{-}39}$= 6.4 Hz, H-40'); 0.74 (12H, d, $J_{35\text{-}34}$ = 7.1 Hz, H-35); 0.67 (12H, d, $J_{35'\text{-}34}$ = 7.1 Hz, H-35').

^{13}C NMR (150 MHz, 10 mM, DMSO-d_6, 25 °C) δ (ppm):172.7 (C-36, COOH); 170.6 (C-30); 155.5 (C-4); 155.2 (C-6); 123.8/123.1 (C-3/C-7); 126.4 (C-28); 96.3 (C-5); 57.2 (C-38); 55.9 (C-4'); 55.4 (C-6'); 50.6 (C-32); 41.3 (C-29); 40.9 (C-33); 31.6 (C-2); 29.8 (C-39); 23.6 (C-35); 22.9 (C-34); 21.7 (C-35'); 19.0 (C-40); 17.9 (C-40').

***trans*-Suc-AAPF-pNA**. ^{1}H NMR (600 MHz, 4.5 mM, D_2O, pH 7.4, 25 °C) δ (ppm): 8.09 (2H, d, $J_{29\text{-}28}$ = 9.2 Hz, H-29); 7.39 (2H, d, $J_{28\text{-}29}$ = 9.2 Hz, H-28); 7.20 (2H, d, $J_{22\text{-}23}$ = 6.9 Hz, H-22); 7.17 (3H, m, H-23/H-24); 4.51 (1H, dd, $J_{19\text{-}20}$ = 8.7 Hz, $J_{19\text{-}20'}$ = 7.1 Hz, H-19); 4.45 (1H, q, $J_{10\text{-}11}$ = 7.0 Hz, H-10); 4.30 (1H, dd, $J_{16\text{-}15}$ = 8.4 Hz, $J_{16\text{-}15'}$ = 5.7 Hz, H-16); 4.15 (1H, q, $J_{6\text{-}7}$ = 7.3 Hz, H-6); 3.65 (2H, dt, $J_{13\text{-}13'}$ = 10.2 Hz, $J_{13\text{-}14/14'}$ = 6.9 Hz, H-13); 3.49 (2H, dt, $J_{13'\text{-}13}$ = 10.2 Hz, $J_{13'\text{-}14/14'}$ = 6.9 Hz, H-13'); 3.12 (1H, dd, $J_{20\text{-}20'}$ = 13.7 Hz, $J_{20\text{-}19}$ = 8.7 Hz, H-20); 3.01 (1H, dd, $J_{20'\text{-}20}$ = 13.7 Hz, $J_{20\text{-}19}$ = 7.1 Hz, H-20'); 2.35 (2H, m, H-2/H-2'); 2.32 (2H, m, H-3/H-3'); 2.13 (1H, m, H-15); 1.87 (2H, m, H-14/H-14'); 1.72 (1H, m, H-15'); 1.23 (3H, d, $J_{7\text{-}6}$ = 7.3 Hz, H-7); 1.21 (3H, d, $J_{11\text{-}10}$ = 7.0 Hz, H-11).

^{1}H NMR (600 MHz, 4.5 mM, DMSO-d_6, 25 °C) δ (ppm): 12.04 (1H, br s, COOH); 10.24 (1H, s, H-26); 8.22 (2H, d, $J_{29\text{-}28}$ = 9.0 Hz, H-29); 8.15 (1H, d, $J_{18\text{-}19}$ = 7.5 Hz, H-18); 8.04 (1H, d, $J_{9\text{-}10}$ = 7.0 Hz, H-9); 8.01 (1H, d, $J_{5\text{-}6}$ = 7.5 Hz, H-5); 7.89 (2H, d, $J_{28\text{-}29}$ = 9.0 Hz, H-28); 7.25 (4H, m, H-22/H-23); 7.19 (1H, m, H-24); 4.60 (1H, m, H-19); 4.48 (1H, m, H-10); 4.26 (2H, m, H-6/H-16); 3.55 (1H, m, H-13); 3.48 (1H, m, H-13'); 3.14 (1H, dd, $J_{20\text{-}20'}$ = 13.7 Hz, $J_{20\text{-}19}$ = 5.1 Hz, H-20); 2.96 (1H, dd, $J_{20'\text{-}20}$ = 13.7 Hz, $J_{20'\text{-}19}$ = 9.6 Hz, H-20'); 2.38 (2H, m, H-2/2'); 2.34 (2H, m, H-3/3'); 1.97 (1H, m, H-15); 1.79 (2H, m, H-14/14'); 1.66 (1H, m, H-15'); 1.16 (3Hd, $J_{7\text{-}6}$ = 7.1 Hz, H-7,); 1.15 (3H, $J_{11\text{-}10}$ = 7.1 Hz, H-11).

^{13}C NMR (150 MHz, 4.5 mM, DMSO-d_6, 25 °C) δ (ppm): 173.8 (C-1); 171.9 (C-8); 171.7 (C-17); 171.0 (C-12); 170.9 (C-25); 170.7 (C-4); 144.8 (C-27); 142.4 (C-30); 137.4 (C-21); 129.1 (C-22); 128.2 (C-23); 126.5 (C-24); 125.0 (C-29); 119.0 (C-28); 59.7 (C-16); 55.0 (C-19); 47.9 (C-6); 46.7 (C-13); 46.4 (C-10); 36.6 (C-20); 29.8 (C-3); 29.1 (C-2); 28.8 (C-15); 24.4 (C-14); 18.1 (C-7); 16.7 (C-11).

***cis*-Suc-AAPF-pNA**. ^{1}H NMR (600 MHz, 4.5 mM, DMSO-d_6, 25 °C) δ (ppm): 10.54 (1H, s, H-26); 8.59 (1H, d, $J_{18\text{-}19}$ = 6.8 Hz, H-18); 8.18 (2H, d, $J_{29\text{-}28}$ = 9.2 Hz, H-29); 7.85 (1H, d, $J_{9\text{-}10}$ = 9.4 Hz, H-9); 7.76 (2H, d, $J_{28\text{-}29}$ = 9.2 Hz, H-28); 4.65 (1H, m, H-19); 4.44 (1H, m, H-16); 4.32 (1H, m, H-6); 4.26 (1H, m, H-10); 3.55 (1H, m, H-13); 3.48 (1H, m, H-13'); 3.08 (2H, m, H-20/20'); 2.06 (1H, m, H-15); 1.93 (1H, m, H-15'); 1.66 (1H, m, H-14/H-14'); 1.43 (1H, m, H-14'/H-14).

Molecular Modeling

A rough structure of **1**-DD was built using Maestro and energy minimized for 5000 steps in implicit water solvent by means of Macromodel (AMBER* force field).[27,28] Setting parameters were kept at their default values. The conformational analysis was then performed on the rotatable bonds of the four dipeptide chains of **1**-DD, while the flattened cone conformation of the resorcin[4]arene moiety was kept frozen. To this end, 10000 steps of the Mixed torsional/Low-mode sampling conformational search implemented in Macromodel (AMBER* force field) were run. The 1000 conformers of **1**-DD endowed with the lowest total energy were stored.

As in a previous work,[7a] the crystallographic structure of ChT was retrieved from the Protein Data Bank under the accession code 1YPH and was prepared for docking with the make_receptor graphical utility implemented in the OEDocking suite.[23] A box volume of 123221 $Å^3$ with dimensions 48.00 x 50.67 x 50.67 Å covering the accessible surface of the ChT catalytic groove was used. Molecular docking of the 1000 conformers of **1**-DD was performed with FRED.

The complex between ChT and the representative docking pose of **1**-DD was energy minimized with Amber12 in a box of explicit water molecules (TIP3P type) buffering 6 Å. The ff12 and the GAFF force fields were used for simulating the protein and the ligand, respectively. During the system preparation with LeaP, the catalytic His57 was parameterized as a Histidine-Delta (HID). The total charge of the system was neutralized by the addition of a Na^+ counterion. First, water molecules were energy minimized for 1000 steps with a steepest-descent algorithm (SD) and subsequent 2000 steps with a conjugate gradient algorithm (CG) while keeping the ChT/**1**-DD complex frozen. Then, the whole system was energy minimized for 1500 steps SD and 6500 steps CG.

Acknowledgements

Authors wish to thank the OpenEye Free Academic Licensing Program for providing a free academic license for molecular modeling and chemoinformatics software.

Notes and references

[a] Dipartimento di Chimica e Chimica Industriale, Università di Pisa, Via G. Moruzzi 3, 56124 Pisa, Italy.
[b] Center for Life Nano Science@Sapienza, Istituto Italiano di Tecnologia, Viale Regina Elena 291, 00161 Roma, Italy.
[c] Dipartimento di Chimica e Tecnologie del Farmaco, Università degli studi di Roma "La Sapienza", piazzale Aldo Moro 5, 00185, Roma.
Electronic Supplementary Information (ESI) available: [Stereochemical characterization of **1**-DD and Suc-AAPF-pNA, Table 6S, Figures 11S and 12S (see manuscript)]. See DOI: 10.1039/b000000x/

1 (a) J. Andreani, R. Guerois, *Arch. Biochem. Biophys.*, 2014, **554**, 65-75; (b) H.-C. Lu, A. Fornili, F. Fraternali, *Expert Rev. Proteomics*, 2013, **10**, 511-520; (c) M. Vidal, M. E. Cusick, A.-L. Barabasi, *Cell*, 2011, **144**, 986-998.
2 (a) Q. Luo, Z. Dong, C. Hou, J. Liu, *Chem. Comm.*, 2014, **50**, 9997-10007; (b) T. Passioura, T. Katoh, Y. Goto, H. Suga, Hiroaki, *Annu. Rev. Biochem.*, 2014, **83**, 727-752.
3 (a) L. L. Kiessling, J. E. Gestwicki, L. E. Strong, *Curr. Opin. Chem. Biol.*, 2000, **4**, 696-703; (b) B. S. Sandanaraj, D. R. Vutukuri, J. M. Simard, A. Klaikherd, R. Hong, V. M. Rotello, S. Thayumanavan, *J. Am. Chem. Soc.*, 2005, **127**, 10693-10698.
4 (a) W. Guo, J. A. Wisniewski, H. Ji, *Bioorg. Med. Chem. Lett.*, 2014, **24**, 2546-2554; (b) L. Jin, W. Wang, G. Fang, *Annu. Rev. Pharmacol. Toxicol.*, 2014, **54**, 435-456; (c) Y. Rew, D. Sun, *J. Med. Chem.*, 2014, **57**, 6332-6341.
5 (a) V. Martos, P. Castreno, J. Valero, J. de Mendoza, *Curr. Opin. Chem. Biol.*, 2008, **12**, 698-706; (b) S. Fletcher Steven; A. D. Hamilton, *Curr. Opin. Chem. Biol.*, 2005, **9**, 632-638.
6 (a) K. D. Daze, T. Pinter, C. S. Beshara, A. Ibraheem, S. A. Minaker, M. C. F. Ma, R. J. M. Courtemanche, R. E. Campbell, F. Hof, *Chem. Sci.*, 2012, **3**, 2695-2699; (b) R. E. Brewster, K. L. Caran, J. S. Sasine, S. B. Shuker, *Curr. Org. Chem.*, 2004, **8**, 867-881.
7 (a) I. D'Acquarica, A. Cerreto, G. Delle Monache, F. Subizi, A. Boffi, A. Tafi, S. Forli, B. Botta, *J. Org. Chem.*, 2011, **76**, 4396-4407; (b) B. Botta, C. Fraschetti, I. D'Acquarica, M. Speranza, F. R. Novara, J. Mattay, C. L. Matthias, *J. Phys. Chem. A*, 2009, **113**, 14625-14629; (c) B. Botta, I. D'Acquarica, G. Delle Monache, D. Subissati, G. Uccello-Barretta, M. Mastrini, S. Nazzi, M. Speranza, *J. Org. Chem.*, 2007, **72**, 9283-9290.
8 F. Sansone, L. Baldini, A. Casnati, M. Lazzarotto, G. Faimani, F. Ugozzoli, R. Ungaro, R. *Proc. Natl. Acad. Sci. U.S.A.*, 2002, **99**, 4842-4847.
9 F. Sansone, L. Baldini, A. Casnati, E. Chierici, F. Ugozzoli, R. Ungaro, *J. Am. Chem. Soc.*, 2004, **126**, 6204-6205.
10 (a) H. S. Park, Q. Lin, A. D. Hamilton, *J. Am. Chem. Soc.*, 1999, **121**, 8; (b) H. S. Park, Q. Lin, A. D. Hamilton, *Proc. Natl. Acad. Sci. U.S.A.*, 2002, **99**, 5105.
11 D. Neuhaus, M. Williamson, in *The Nuclear Overhauser Effect in structural and conformational analysis*. WCH Publishers Inc., Cambridge, 1989.
12 G. Valensin, G. Sabatini, E. Tiezzi, in *Advanced Magnetic Resonance Techniques in Systems of High Molecular Complexity*, ed. N. Niccolai and G. Valensin, Birkhauser Inc., Boston, 1986, pp. 69–76.
13 (a) A. Macchioni, G. Ciancaleoni, C. Zuccaccia, D. Zuccaccia, P. A. Gale, J. W. Steed, in *Supramolecular Chemistry: From Molecules to Nanomaterials*, ed. P. Gale, J. Steed, Wiley and Sons, Chichester, U.K., 2012, Vol. 2, pp 319-330; (b) G. A. Morris, Diffusion-ordered spectroscopy. In Multidimensional NMR Methods for the Solution State; Morris, G. A.; Emsley, J. W., Eds.; Wiley and Sons, Chichester, U.K., 2010, pp 515-532; (c) G. A. Morris, in *Encyclopedia of Nuclear Magnetic Resonance*, ed. D. M. Grant, R. K. Harris, Wiley and Sons, Chichester, U.K., 2002, Vol 9, pp 35–44.
14 I. D'Acquarica, A. Calcaterra, F. Sacco, G. Uccello-Barretta, F. Balzano, F. Aiello, A. Tafi, B. Botta, *Chirality*, 2013, **25**, 840-851.
15 (a) K. Lang, F. X. Schmid, *Nature*, 1988, **331**, 453-455; (b) L. T. Kakalis, I. M. Armitage, I. M., *Biochemistry*, 1994, **33**, 1495-1501; (c) J. L. Kofron, P. Kuzmič, V. Kishore, E. Colón-Bonilla, D. H. Rich, *Biochemistry*, 1991, **30**, 6127-6134; (d) J. J. Siekierka, S. H. Y. Hung, M. Poe, C. S. Lin, N. H. Sigal, *Nature*, 1989, **341**, 755-757.
16 G. Uccello-Barretta, E. Domenici, C. Bertucci, P. Salvadori, *J. Am. Chem. Soc.*, 1991, **113**, 7017-7019.
17 C. Rossi, A. Donati, C. Bonechi, G. Corbini, R. Rappuoli, E. Dreassi, P. Corti, *Chem. Phys. Lett.*, 1997, **264**, 205-209.
18 (a) G. Corbini, S. Martini, C. Bonechi, M. Casolaro, P. Corti, C. Rossi, *J. Pharm. Biomed. Anal.*, 2006, **40**, 113-121; (b) S. Martini, C. Bonechi, M. Casolaro, G. Corbini, C. Rossi, *Biochem. Pharm.*, 2006, **71**, 858-864.
19 D. M. Blow, J. J. Birktoft, B. S. Hartley, *Nature*, 1969, **221**, 337-340.
20 (a) G. Uccello-Barretta, F. Balzano, F. Pertici, L. Jicsinszky, G. Sicoli, V. Schurig, *Eur. J. Org. Chem.*, 2008, 1855-1863; (b) E. J. Cabrita, S. Berger, *Magn. Reson. Chem.*, 2001; **39**, S142-S148.
21 B. Botta, M. Cassani, I. D'Acquarica, D. Misiti, D. Subissati, G. Delle Monache, *Curr. Org. Chem.*, 2005, **9**, 337-355.
22 A. G. S. Högberg, *J. Am. Chem. Soc.*, 1980, **102**, 6046-6050.
23 A. G. S. Högberg, *J. Org. Chem.*, 1980, **45**, 4498-4500.
24 (a) FRED version 3.0.1 OpenEye Scientific Software, Santa Fe, NM. http://www.eyesopen.com; (b) M. McGann, FRED pose prediction and virtual screening accuracy. *J. Chem. Inf. Model.*, 2011, **51**, 578-596.
25 D. A. Case, T. A. Darden, T. E. Cheatham, III, C. L. Simmerling, J. Wang, R. E. Duke, R. Luo, R. C. Walker, W. Zhang, K. M. Merz, B. Roberts, S. Hayik, A. Roitberg, G. Seabra, J. Swails, A. W. Goetz, I. Kolossváry, K. F. Wong, F. Paesani, J. Vanicek, R. M. Wolf, J. Liu, X. Wu, S. R. Brozell, T. Steinbrecher, H. Gohlke, Q. Cai, X. Ye, J. Wang, M.-J. Hsieh, G. Cui, D. R. Roe, D. H. Mathews, M. G. Seetin, R. Salomon-Ferrer, C. Sagui, V. Babin, T. Luchko, S. Gusarov, A. Kovalenko, and P. A. Kollman 2012, AMBER 12, University of California, San Francisco.
26 R. Freeman, S. Wittekoek, *J. Magn. Reson.*, 1969, **1**, 238-276.
27 Maestro, version 9.2, Schrödinger, LLC, New York, NY, 2011.
28 MacroModel, version 9.9, Schrödinger, LLC, New York, NY, 2011.